ACS Chemical Neuroscience

Research Article

pubs.acs.org/chemneuro

Model for High-Throughput Screening of Multitarget Drugs in Chemical Neurosciences: Synthesis, Assay, and Theoretic Study of Rasagiline Carbamates

Nerea Alonso,[†] Olga Caamaño,[†] Francisco J. Romero-Duran,[†] Feng Luan,[‡,§] M. Natália D. S. Cordeiro,[‡] Matilde Yañez,[∥] Humberto González-Díaz,*[,⊥,#] and Xerardo García-Mera*[,†]

[†]Department of Organic Chemistry, Faculty of Pharmacy, University of Santiago de Compostela (USC), 15782, Santiago de Compostela, Spain

[‡]REQUIMTE/Department of Chemistry and Biochemistry, University of Porto, 4169-007, Porto, Portugal

[§]Department of Applied Chemistry, Yantai University, Yantai 264005, People's Republic of China

[∥]Department of Pharmacology, Faculty of Pharmacy, USC, 15782, Santiago de Compostela, Spain

[⊥]Departament of Organic Chemistry II, University of the Basque Country UPV/EHU, 48940, Leioa, Spain

[#]IKERBASQUE, Basque Foundation for Science, 48011, Bilbao, Spain

Supporting Information

ABSTRACT: The disappointing results obtained in recent clinical trials renew the interest in experimental/computational techniques for the discovery of neuroprotective drugs. In this context, multitarget or multiplexing QSAR models (mt-QSAR/mx-QSAR) may help to predict neurotoxicity/neuroprotective effects of drugs in multiple assays, on drug targets, and in model organisms. In this work, we study a data set downloaded from CHEMBL; each data point (>8000) contains the values of one out of 37 possible measures of activity, 493 assays, 169 molecular or cellular targets, and 11 different organisms (including human) for a given compound. In this work, we introduce the first mx-QSAR model for neurotoxicity/neuroprotective effects of drugs based on the MARCH-INSIDE (MI) method. First, we used MI to calculate the stochastic spectral moments (structural descriptors) of all compounds. Next, we found a model that classified correctly 2955 out of 3548 total cases in the training and validation series with Accuracy, Sensitivity, and Specificity values > 80%. The model also showed excellent results in Computational-Chemistry simulations of High-Throughput Screening (CCHTS) experiments, with accuracy = 90.6% for 4671 positive cases. Next, we reported the synthesis, characterization, and experimental assays of new rasagiline derivatives. We carried out three different experimental tests: assay (1) in the absence of neurotoxic agents, assay (2) in the presence of glutamate, and assay (3) in the presence of H_2O_2. Compounds **11** with 27.4%, **8** with 11.6%, and **9** with 15.4% showed the highest neuroprotective effects in assays (1), (2), and (3), respectively. After that, we used the mx-QSAR model to carry out a CCHTS of the new compounds in >400 unique pharmacological tests not carried out experimentally. Consequently, this model may become a promising auxiliary tool for the discovery of new drugs for the treatment of neurodegenerative diseases.

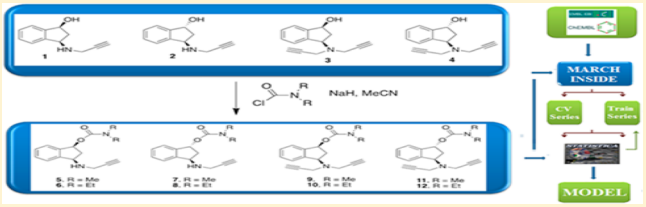

KEYWORDS: *Neurodegenerative diseases, drug-target networks, rasagiline derivatives, CHEMBL, multitarget QSAR, multiplexing assays, high-throughput screening, moving averages, spectral moments, Markov chains*

Alzheimer's disease (AD),[1] vascular dementia (VD),[2] Parkison's disease (PD),[3] amyotrophic lateral sclerosis (ALS),[4] Huntington's disease (HD),[5] and other neurodegenerative diseases are some of the hot topics in drug discovery nowadays. They are characterized by prominent age-related neurodegeneration in selectively vulnerable neural systems. The genes causing hereditary forms of AD, PD, and ALS have been identified. Nonetheless, the mechanisms of the neuronal degeneration in these diseases remain unknown to an important extent.[6] In addition, the disappointing results of some recent clinical trials have renewed the need for complementary techniques in the discovery of neuroprotective drugs.[7] In this sense, multitarget/multiplexing techniques, used to measure or predict neurotoxicity/neuroprotective profiles of drugs, may be useful in the discovery of new lead compounds against neurodegenerative diseases.[8] On the other hand, the large number of experimental results reported by different groups worldwide has led to the accumulation of huge amounts of information in large databases. This determines, in turn, the need of new algorithms to perform data mining of these databases. CHEMBL is more likely the largest and one of the

Received: May 21, 2013
Accepted: July 15, 2013
Published: July 15, 2013

most useful public databases for the development of drug discovery techniques (https://www.ebi.ac.uk/chembldb).[9,10]

In our opinion, computational chemistry techniques based on quantitative structure−property relationships (QSAR) may play an important role in chemical neurosciences, in this sense. For instance, Mueller et al. reported in *ACS Chemical Neuroscience* the identification of mGluR subtype 5 potentiators using QSAR models for computational chemistry simulation of high-throughput screening (CCHTS) experiments.[11] Unfortunately, most current QSAR techniques can predict the probable result of one drug in one specific assay. Nevertheless, recently developed multitarget/multiplexing QSAR models (mt-QSAR/mx-QSAR) may become a useful tool in this regard. These methods are especially powerful when we need to process very large collections of compounds assayed against multiple molecular or cellular targets in different assay conditions (c_j) as is the case of CHEMBL.[12,13] We can use different software to calculate molecular descriptors and develop mt-QSAR or mx-QSAR models: DRAGON,[14,15] MOE,[16] TOPS-MODE,[17−19] CODESSA,[20−22] TOMOCOMD,[23,24] or MARCH-INSIDE (MI),[25−27] software used in this work. For instance, we used MI to develop different mt-QSAR classifiers/web-servers such as MIND-BEST[28] or NL MIND-BEST.[29] The first two use MI only, but the third combines DRAGON and MI to calculate descriptors for drugs and proteins, respectively. Another mt-QSAR/mx-QSAR strategy uses only drug molecular descriptors and incorporate moving average terms into the equation (see Methods section). For instance, we developed an mt-QSAR for tyrosine kinase inhibitors using the TOPS-MODE[30] method. Moreover, Speck-Planche and co-workers combined DRAGON and TOPS-MODE to seek mt-QSAR/mx-QSAR models for CCHTS.[31−36]

In any case, this is a new branch of QSAR and it does not seem there are many reports of multipurpose mx-QSAR models for testing neurotoxicity/neuroprotective effects of drugs. We reported an mx-QSAR model for multiplexing assays of anti-Alzheimer compounds using MI. However, the model predicts only assays of GSK-3 inhibitors in vitro, in vivo, and in different cellular lines.[37] In the present project, we used MI for the first time to find an mx-QSAR model for neuroprotective effects of drugs. We trained and validated the model with nonoverlapping training and external prediction data series obtained from CHEMBL. In addition, we simulated a CCHTS of >4000 positive cases with excellent results. Last, we exemplified the use of the new mx-QSAR model with an unreported case study. To this end, organic synthesis, characterization, and biological assay of new rasagiline derivatives were reported for the first time. Rasagiline is a promising drug for the treatment of PD.[38,39] Subsequently, we predicted the most probable results for these compounds in a CCHTS experiment with >400 assays not carried out experimentally in this work. Figure 1 presents a general workflow of the steps given to develop and use the model.

1. RESULTS AND DISCUSSION

1.2. Model of Drug Neuroprotective Effects Based on Markov Spectral Moments. *1.2.1. Training and Validation of the Model.* In this work, we report the first mx-QSAR model with an output variable $S_i(c_j)$ able to discriminate whether a compound may give a positive result $(A_i(m_j) = 1)$ or not $(A_i(m_j) = 0)$ in different multiplexing assay conditions c_j. The output $S_i(c_j)$ of our multiplexing model depends on both chemical structure of the ith drug d_i and the set of conditions

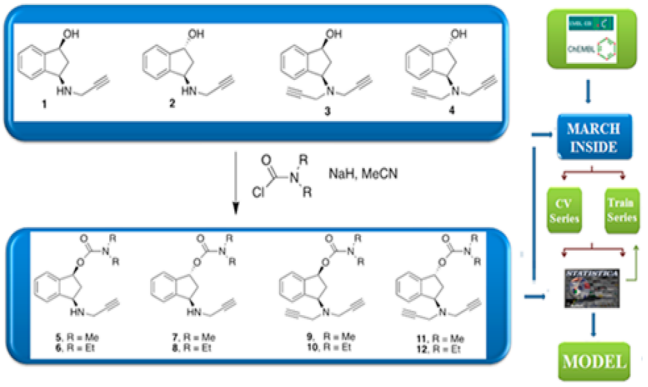

Figure 1. Synthesis of compounds **5**−**12** and development/application of the mx-QSAR model.

selected to perform the biological assay (c_j). In consonance, the mx-QSAR should predict different probabilities if we change the organisms (o_t), the biological assays (a_u), the molecular/cellular target (t_e), or the standard experimental parameter measured (s_x), for the same compound.[40−43] The best mx-model found in this work was

$$S_i(c_j) = 1.139556 - 0.403994p(c_1)\pi_5^i + 0.199322\Delta\pi_5^i(s_x) + 0.434889\Delta\pi_5^i(a_u) - 0.020189\Delta\pi_5^i(o_t) - 0.001660\Delta\pi_1^i(t_e)$$

$$N = 2661, \quad R_c = 0.72, \quad \chi^2 = 1913.007, \quad p < 0.005 \tag{1}$$

The first term in the equation, $p(c_1)\pi_5^i$, codifies the quality of the input data and the effect of the chemical structure of the drug (π_5^i) over the final biological activity predicted. The model presented in the present work is based on the fifth order spectral moments, which are equal to $\pi_5^i = \mathrm{Tr}[(^1\mathbf{\Pi})^5]$ and have been calculated with the MI software.[25−27] The operator Tr is the trace (sum of elements in the main diagonal) of the Markov matrix ($^1\mathbf{\Pi}$). The elements of the matrix $^1\mathbf{\Pi}$ used are atom−atom electron delocalization probabilities, and the atomic weights are standard electronegativities. The statistical parameters for the above equation in training are as follows: Number of cases used to train the model (N), canonical regression coefficient (R_c), chi-square (χ^2), and p-level.[41,42] The probability cutoff for this classification model is $^1p_i(c_j) > 0.5 \rightarrow A_i(c_j) = 1$. It means that the ith drug (d_i) predicted by the model with probability >0.5 is expected to give a positive outcome in the jth assays carried out under the given set of conditions c_j. This mx-QSAR has excellent goodness-of-fit statistics in both training and external validation series with sensitivity (Sn), specificity (Sp), and accuracy (Ac) > 80% (see Table 1). Values higher than 75% are acceptable for QSAR classification models, according to previous reports.[43−51]

We used the probability $p(c_1)$ = 1.0, 0.75, or 0.5 for data values reported in CHEMBL as curated at an expert, intermediate, or autocuration level, respectively. This parameter accounts for the accuracy (c_j) of the input experimental data for the assay carried out in c_j conditions. The parameter π_5^i quantifies the topological information of chemical structure and the physicochemical properties of the atoms in the molecule. We can write the same equation in an expanded form:

Table 1. Overall Results of the mx-QSAR Classification Model

subset	stat[a]	%	groups	$C_i(m_j)_{pred} = 0$	$C_i(m_j)_{pred} = 1$	ref
MARCH-INSIDE model						
training	Sp	84.6	$C_i(m_j)_{obs} = 0$	**1172**	214	this work
	Sn	82.4	$C_i(m_j)_{obs} = 1$	224	**1051**	
	Ac	83.5	total			
CV	Sp	83.3	$C_i(m_j)_{obs} = 0$	**385**	77	
	Sn	81.6	$C_i(m_j)_{obs} = 1$	78	**347**	
	Ac	82.5	total			
HTS	Sn	90.6	$C_i(m_j)_{obs} = 1$	**4315**	446	
TOPS-MODE model						
training	Sp	81.3	$C_i(m_j)_{obs} = 0$	**1533**	352	43
	Sn	98.0	$C_i(m_j)_{obs} = 1$	36	**1762**	
	Ac	89.5	total			
CV	Sp	81.0	$C_i(m_j)_{obs} = 0$	**513**	120	
	Sn	97.7	$C_i(m_j)_{obs} = 1$	14	**585**	
	Ac	89.1	total			

[a]Statistics: Sensitivity = Sn = Positive **Correct**/Positive Total; Specificity = Sp = Negative **Correct**/Negative Total; Accuracy = Ac = Total **Correct**/Overall Total.

$$S_i(c_j) = 1.139556 - 0.403994p(c_1)\pi_5{}^i + 0.199322 [\pi_5{}^i(s_x) - p(s_x)\langle\pi_5(s_x)\rangle] + 0.434889 [\pi_5{}^i(a_u) - p(a_u)\langle\pi_5(a_u)\rangle] - 0.020189 [\pi_5{}^i(o_t) - p(o_t)\langle\pi_5(o_t)\rangle] - 0.001660 [\pi_5{}^i(t_e) - p(t_e)\langle\pi_5(t_e)\rangle]$$

$$N = 2661, \quad R_c = 0.72, \quad \chi^2 = 1913.007, \quad p < 0.005 \tag{2}$$

A value of ${}^1p_i(c_j) > 0.5$ predicts a high response $S_i(c_j)$ for this compound with respect to different standard parameters, targets, assays, or even different organisms. To this end, we only have to substitute in the equation the value of $\pi_5{}^i$ of the compound and the respective values $p(c_j)\langle\pi_5{}^i(m_j)\rangle$ already tabulated; see Table 2.

Table 3 reports the detailed results obtained with the model for different c_j. The prediction of results of assays in humans with respect to other species is of major interest in this sense.[43] In fact, the model predicts 85.1% of the 1675 assays in *Homo sapiens* and 79.6% of the 1464 assays in *Rattus norvegicus*. Consequently, this equation may become a tool to extrapolate experimental results from laboratory animals to humans. The scale of the experimental measure influences the accuracy of the model, for example, for log K_i values Ac = 100% but K_i cases Ac = 61.4%.

In any case, Table 3 illustrates that we are in the presence of a very powerful model with multiple outputs for the same compound. For instance, the model correctly predicted 91.7% of the 1581 values of $-\log(IC_{50})$ (nM), 100% of the 384 values of selectivity, 93.7% of the 222 values of relative activity (%), 100% of the 105 cases of selectivity ratio, and so forth. The previous aspects remind of the multiplexing nature of the model. However, we should not forget that this model is also a very powerful mt-QSAR able to predict the probability with which a compound may interact with a high number of targets in the nervous system. For instance, the model correctly predicted 904, 126, and 122 interactions of different drugs with brain, endothelial, or inducible nitric-oxide synthases (iNOS) with Ac (%) = 97.4, 81.0, and 83.6%, respectively. The model also predicted correctly more than 250 drug−protein interactions for different neuronal acetylcholine receptors with Ac(%) = 70−100% in all cases; see Table 3.

1.2.2. Comparison with Another mx-QSAR Model. An interesting exercise is the comparison of the present model with other models reported in the literature for a similar purpose. To the best of our knowledge, there is only one mx-QSAR model reported in the literature with similar capabilities. The model was published this year by our group. The equation of this model is the following:[43]

$$S_i(c_j) = (-7.01 \times 10^{-4})p(c_j)\mu_5{}^i - (7.84 \times 10^{-4})\Delta\mu_5{}^i(s) - (2.93 \times 10^{-4})\Delta\mu_5{}^i(a) + (1.16 \times 10^{-4})\Delta\mu_5{}^i(o) + (2.84 \times 10^{-4})\Delta\mu_5{}^i(t) + 4.198684$$

$$N = 3683, \quad R_c = 0.7, \quad S_n = 98.0, \quad S_p = 81.3, \quad Ac = 89.5 \tag{3}$$

A close inspection of this equation reveals some similarities and differences between both models. In both models the molecular descriptors ($D_k{}^i$) used to codify the structure of compounds (see Methods section) are spectral moments of a molecular matrix. The model reported in the previous work was developed using the spectral moment $\mu_5{}^i$ calculated with the TOPS-MODE approach.[43] These spectral moments, $\mu_k{}^i = Tr[({}^1\mathbf{B})^k]$ are descriptors based on the bond adjacency matrix (${}^1\mathbf{B}$). Specifically, we used only one descriptor, the fifth order spectral moment $\mu_5{}^i$. In this case, we used standard distances of chemical bonds and not atomic weights. Apart from it, the general formulations of both models are similar. In both cases, we used Moving Average terms to quantify the deviations of the structure of one compound from subsets of compounds with a positive outcome in different conditions c_j.

Both models show a very good Specificity (Sp) both in training and validation. However, the TOPS-MODE model shows better values of Sensitivity both in training and validation. Also, the values of $p(c_j)$, $\langle\pi_5{}^i(c_j)\rangle$, and $\langle\mu_5{}^i(c_j)\rangle$ are different for different subsets c_j. These similarities/differences between both models may be discussed considering the differences in the respective data sets used to develop and validate them. There are many aspects that determined that both data sets were not similar. In the first model we used only

Table 2. Selected Examples of Average Values for Different Targets, Measures, and Organisms

MEASURE (s_x) (unit)	n_{tot}	$p_1(s_x)$	$p_1(s_x)\langle\pi_5(s_x)\rangle$	MEASURE (s_x) (unit)	n_{tot}	$p_1(s_x)$	$p_1(s_x)\langle\pi_5(s_x)\rangle$
%max (%)	20	0.20	2.08	log K_i	124	0.58	2.24
activity	8	0.63	9.63	$-\log(IC_{50})$ (nM)	2438	0.88	5.98
activity (%)	222	0.47	4.62	MTT reduction (%)	11	0.36	1.34
activity (nM)	98	0.95	3.67	nNOS activity (%)	36	0.69	4.56
damage score	8	0.25	0.93	pA2	34	0.06	0.32
decrease (%)	5	0.80	4.29	PCMA antagonism	84	0.31	1.59
dopamine release (%)	299	0.43	1.56	pD2	35	0.57	2.39
EC_{50} (nM)	2149	0.92	4.80	ratio	108	0.29	1.75
efficacy (%)	12	0.50	1.97	ratio (nM)	56	0.57	1.77
efficiency (%)	14	0.79	3.32	ratio K_i	12	0.17	1.00
inhibition (%)	193	0.48	2.76	relative potency	11	0.36	2.43
inhibition (nM)	7	0.71	3.39	selectivity	486	0.21	1.51
K_i (nM)	1501	0.94	4.59	selectivity ratio	166	0.37	2.69
ORGANISM (o_t)	n_{tot}	$p_1(o_t)$	$p_1(o_t)\langle\pi_5(o_t)\rangle$	ORGANISM (o_t)	n_{tot}	$p_1(o_t)$	$p_1(o_t)\langle\pi_5(o_t)\rangle$
H. sapiens	4854	0.84	7.50	*B. taurus*	77	0.27	2.86
R. norvegicus	2852	0.70	5.57	*C. porcellus*	20	0.80	5.58
F. catus	10	0.70	5.75	*H. virescens*	5	1.00	12.94
M. musculus	241	0.72	6.89	*M. domestica*	15	1.00	7.36
T. californica	19	0.58	5.19	*C. elegans*	2	0.50	5.58
Gerbillinae sp.	8	0.25	1.37	*D. melanogaster*	2	0.50	5.58

TARGET ID	n_{tot}	$p_1(t_e)$	$p_1(t_e)\langle\pi_5(t_e)\rangle$	TARGET NAME (t_e)
1907589	31	0.74	4.62	neuronal AChR; alpha4/beta2
1883	43	0.84	7.39	neuronal AChR protein beta-2 subunit
4980	142	0.78	6.35	neuronal AChR protein alpha-7 subunit
3461	126	0.90	6.05	neuronal AChR protein alpha-10 subunit
2658	104	0.87	5.80	neuronal AChR protein beta-4 subunit
2584	79	0.84	5.30	neuronal AChR protein alpha-2 subunit
1907596	67	0.45	2.83	neuronal AChR; alpha4/beta2
4960	79	0.84	5.30	neuronal AChR protein alpha-5 subunit
3568	859	0.65	4.99	nitric-oxide synthase, brain
3048	403	0.63	5.63	nitric-oxide synthase, brain
3251	1000	0.92	7.27	nuclear factor NF-kappa-B p105 subunit
5533	1000	0.92	7.27	nuclear factor NF-kappa-B p65 subunit
304	16	1.00	7.50	norepinephrine transporter
313	71	0.45	3.45	serotonin transporter
4187	47	0.98	9.80	sodium channel protein type II alpha subunit
1920	46	1.00	8.89	GABA receptor beta-2 subunit
341	38	1.00	8.87	GABA receptor alpha-2 subunit
3772	16	0.88	5.02	MGluR 1
5137	32	1.00	7.71	MGluR 2
2888	29	0.97	7.68	MGluR 3
2736	13	0.85	4.74	MGluR 4
3227	16	0.81	4.65	MGluR 5
3777	13	0.62	3.48	MGluR 7
1907608	24	1.00	11.22	glutamate NMDA receptor

4915 data points = 3683 training + 1232 validation cases).[42] Nevertheless, the data set used in the present work is notably larger and includes 309 data points = 2661 training + 887 validation + 4761 positive cases for the CCHTS experiment. This notable difference in the data sets used is due to the different aims of both works. In the first work, we were more interested in the possibility of training and validation of this type of mx-QSAR model, regardless of the software used. In this second work, we are more interested in the possible use of this type of models for CCHTS of compounds with a final positive outcome. It means that the TOPS-MODE was not tested on a CCHTS simulation yet (with a rather large series of compounds), such as the case of the MI model. That is why the number of cases used in this second work with MI is notably larger due to the use/incorporation of a high number of positive cases (4761 in total) for the CCHTS simulation experiment. It should be noted the high value of Sn = 90.6, obtained with the present model in the CCHTS experiment despite the fact we previously used the double of positive cases than in training series.

1.3. Experimental–Theoretical Study of New Neuroprotective Drugs. *1.3.1. Experimental Assay of Neuroprotective Effects of New 1,3-Rasagiline Derivatives.* The compounds (**5**, **6**, **7**, **8**, **9**, **10**, **11**, and **12**) were synthesized according to the strategy given in Figure 1; see also Methods section. The synthesized compounds (**5**–**12**) were subjected to an initial study to determine their neuroprotective capacity in both the absence and presence of neurotoxic agents, using

Table 3. Number of Cases versus Accuracy for Some Organisms, Experimental Parameters, or Targets

ORGANISM	n_1	Ac(%)	ORGANISM	n_1	Ac(%)
Homo sapiens	1675	85.1	*Cavia porcellus*	40	22.5
Rattus norvegicus	1464	79.6	*Felis catus*	18	44.4
Mus musculus	168	76.2	*Gerbillinae*	12	50.0
Bos taurus	56	100	*Torpedo californica*	11	72.7
MEASSURE	n_1	Ac(%)	MEASSURE	n_1	Ac(%)
$-\log(IC_{50})$ (nM)	1581	91.7	nNOS activity (%)	36	58.3
selectivity	384	100	pA2	32	100
dopamine release (%)	299	56.5	ratio (nM)	24	100
activity (%)	222	93.7	%max (%)	20	80.0
inhibition (%)	193	65.8	NO formation (%)	18	66.7
EC_{50} (nM)	174	9.8	pD2	15	100
selectivity ratio	105	100	efficiency (%)	14	50.0
K_i (nM)	83	61.4	Kup (mL min^{-1} g^{-1})	13	61.5
ratio	77	97.4	conc (% dose g^{-1})	12	100
PCMA antagonism	58	100	efficacy (%)	12	50.0
log K_i	52	100	MTT reduction (%)	11	63.6
$-\log(IC_{50})$	39	100	ratio K_i	10	100
TARGET NAME				n_1	Ac(%)
nitric-oxide synthase (bNOS), brain				904	94.7
nitric-oxide synthase (eNOS), endothelial				126	81.0
nitric-oxide synthaseb(iNOS), inducible				122	83.6
neuronal acetylcholine receptor protein beta-2 subunit				59	74.6
neuronal acetylcholine receptor protein beta-4 subunit				57	73.7
neuronal acetylcholine receptor protein alpha-3 subunit				57	73.7
neuronal acetylcholine receptor protein beta-3 subunit				56	73.2
neuronal acetylcholine receptor protein alpha-7 subunit				54	72.2
neuronal acetylcholine receptor; alpha3/beta4				19	100
neuronal acetylcholine receptor; alpha4/beta2				51	100
nuclear factor NF-kappa-B p105 or p65subunit				154	100
sodium channel protein type I, II, or III, alpha subunit				63	100
glutamate [NMDA] receptor subunits epsilon 1, 2, 3, z1, or 3A				54	100
acetylcholine receptor protein beta chain				52	75.0
mGluRs 1, 2, 3, 4, 5, 7, or 8				52	100
melanin-concentrating hormone receptor 1				50	100
serotonin transporter				39	100
GABA receptor alpha-2 subunit				38	100
GABA receptor gamma-2 subunit				38	100
alpha adrenergic receptors 1a, 1b, 1d				27	100
GABA transporter 3				23	82.6
GABA transporter 1				23	82.6
betaine transporter				23	82.6

MTT method to determine cell viability, given by the number of cells present in the culture. The ability of cells to reduce MTT is an indicator of mitochondrial integrity and its functional activity is interpreted as a measure of cell viability. For instance, Wang et al. used this method to show that Exendin-4 improved rat cortical neuron survival under oxygen/glucose deprivation through PKA pathway.[52]

Herein, we carried out three types of assays in cultured neurons of embryonic motor corteces of of fetal Sprague–Dawley rats at embryonic day 19 of gestation. All results are expressed as mean ± SEM of at least three independent experiments (Table 4). First, we studied the ability to induce a neuroprotective effect in the absence of any neurotoxic stimulus. Second, the neuroprotective/citotoxicity effect of

Table 4. Neuroprotective Ability of the New Carbamates of 1,3-Rasagiline Derivatives

n	Formula	Prot. [a] (%)	SEM	Glut. [b] (%)	SEM	H_2O_2 [c] (%)	SEM
5	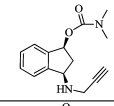	21.2	8.5	-3.8	5.2	-9.3	1.8
6	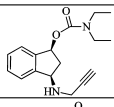	5.0	4.4	-4.0	5.6	-6.8	1.2
7	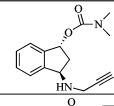	-1.8	2.2	6.7	3.1	-2.5	4.3
8	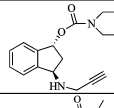	-0.6	2.7	11.6	4.3	-0.1	7
9	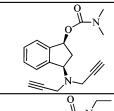	2.8	1.8	-1.6	5.0	15.4	2.3
10	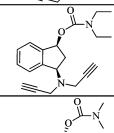	0	5	3.5	3.0	6.2	3.7
11	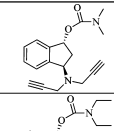	27.4	4.1	7.6	5.0	9.8	2.8
12	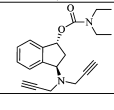	18.2	5.9	4.3	2.0	10.2	2.1

[a]Percent protection (comp 5 μM), in the absence of neurotoxic agents. [b]Percent protection (comp 5 μM) against Glutamate 100 μM. [c]Percent protection (comp 5 μM) against H_2O_2 100 μM.

the compound was studied in the presence of glutamate that causes a pathological process in which the neurons are damaged, ultimately leading to apoptosis. Finally, we examined the ability of the synthesized compounds to protect neurons from damage caused by H_2O_2. The results clearly differentiate mono from dipropargyl derivatives. In the first group, 1,3-*cis* derivatives (**5** and **6**) show interesting values of neuroprotection in the absence of neurotoxic stimuli but remain inactive in the presence of both glutamate and H_2O_2.

However, 1,3-*trans* derivatives (**7** and **8**) showed significant values in the presence of glutamate. In the group of the *N*,*N*-dipropargyl derivatives of rasagiline (**9**–**12**), all the compounds have significant neuroprotective activity against H_2O_2-induced aggression. They also showed some activity against glutamate-induced aggression. Furthermore, both 1,3-*trans* derivatives (**11** and **12**) have important values of neuroprotection, 27.4% and 18.2%, respectively, in the absence of any neurotoxic stimulus. In closing, compounds **11** and **12** not only exhibit neuroprotective activity in the three types of tests, but also indicate that they are highly neuroprotective in the absence of neurotoxic stimuli and have interesting neuroprotective activity in the presence of neurotoxic stimuli. This is depicted graphically in Figure 2.

1.3.3. Prediction of Multiplexing Outcomes of New Neuroprotective Drug in Other Assays. The 3-OH, 3-OAc, and 3-OBz rasagiline derivatives synthesized and experimentally assayed by our group were not very active against some of the expected targets.[28] This situation encouraged us to study the possible neuroprotective activity of our compounds directly in

dx.doi.org/10.1021/cn400111n | ACS Chem. Neurosci. 2013, 4, 1393–1403

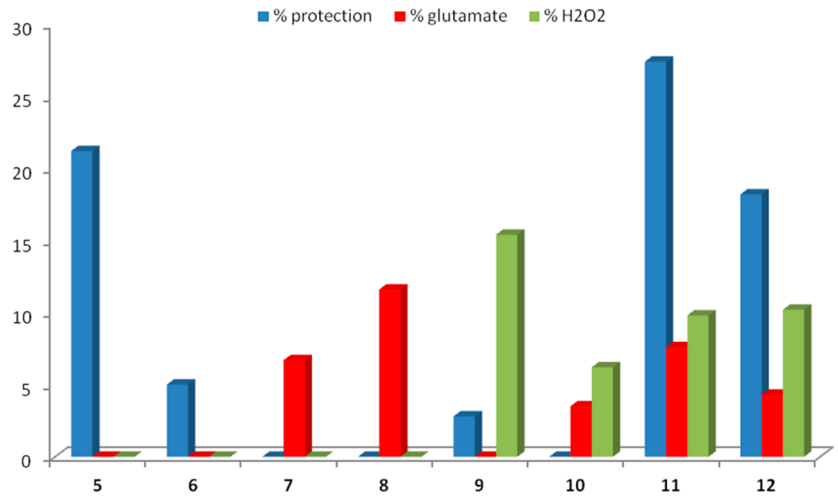

Figure 2. Neuroprotective ability of the compounds tested in this work.

the neuronal culture. In fact, 3-OH, 3-OAc, and 3-OBz rasagiline derivatives were found to present interesting neuroprotective effects in experimental assays.[43] In addition, we were able to predict a high probability of interaction of these compounds with multiple targets of interest in chemical neurosciences such as the metabotropic glutamate receptor (mGluR), the glutamate receptor, the neuronal acetylcholine receptor, and the muscarinic acetylcholine receptor.[43] Using the new model, we performed a CCHTS of the new compounds in several assays not carried out experimentally in this work. We performed the prediction with the 12 new compounds assayed experimentally in the previous section. Consequently, we were able to predict > 11 000 = 12 × 500 theoretical results for the assay of these 12 compounds in >500 assays. However, our discussion will be focused herein only on compound **11**. Compound **11** showed the highest neuroprotective effect in the experiments carried out herein (previous section). The present model does not predict high probabilities for compound **11** such as MAO A/B or AChE inhibitor. Both experimental neuroprotective effect and negative prediction for MAO and Ach coincide with our previous experimental results for 3-OH, 3-OAc, and 3-OBz rasagiline derivatives.

Interestingly, the model has predicted a very high probability $p_1(m_j)$ of activity for compound **11** against different receptors. These predictions point brain iNOS as the most probable target of this compound (see Table 5). The model predicts a positive result for compound **11** in a total of 20 different assays based on this enzyme with values of ${}^1p_i(c_j)$ within the range: 1−0.73. A very recent result claims that Fimasartan, an antihypertension drug, suppressed iNOS expressions via nuclear factor-kappa B and activator protein-1 inactivation.[53] This may be in concordance with the prediction of a $p_1(m_j)$ = 0.78 for compound **11** in assay ChEMBL1613870 that involves Nuclear factor NF-kappa-B p105 subunit. However, the model also predicts positive results for this compound in different assays based on other targets. For instance, the model predicts a positive result for this compound in at least three assays for mGluR and four assays for GABA receptors. Other receptors appear only in one or two cases. These results may indicate a certain probability that compound **11** is a multitarget ligand. In general, the synthesis and assay of multitarget ligands is a promising field in chemical neurosciences. For instance, ITH33/IQM9.21 is a novel compound belonging to a family of glutamic acid derivatives, which was very recently synthesized and assayed under the hypothesis implying that multitarget ligands may provide more efficient neuroprotection than single-targeted compounds.[54] Specifically, an interesting direction is that of searching novel multitarget compounds with neuroprotective effect among the derivatives of rasagiline. Youdim reported a study about Ladostigil (*N*-propargyl-3*R*-aminoindan-5-yl)-ethyl methylcarbamate) and series of multitarget drugs (M30, HLA-20 series) which inhibit AChE, brain MAO A/B, and/or are brain permeable iron chelators and inhibitors of MAO.[55] Conn and co-workers[56−59] have largely discussed the importance of the development of new allosteric modulators of mGluR, but also of the muscarinic receptor, and GPCRs in general. In fact, Csermely et al.[60,61] have recently edited a special issue with different research groups, reviewing this topic and related concepts. In one of these papers, Menniti et al. [62] discussed about the action of allosteric modulators of receptors like AMPA, NMDA, and mGluR in glutamatergic networks for the treatment of schizophrenia. It is expected that network-based tools may be applied for the discovery of new drugs including allo-network drugs.[63−65] All these results led us to prepare and assay the carbamate derivatives of 3-hydroxy-rasagiline in the present work and also to predict their possible interaction with many of these receptors of relevance in glutaminergic networks.

2. CONCLUSIONS

With the MARCH-INSIDE approach, we can seek mx-QSAR models able to fit very large and complex data obtained in multiplexing assays of neuroprotective drug candidates in different assay conditions, targets, and organisms. These models are useful to carry out "in silico" HTS of drugs. New carbamate derivatives of 3-OH rasagiline may be prepared with interesting neuroprotective effects. The new models can predict for the compounds a high number of other pharmacological outcomes not determined experimentally. Last, the new model is able to reconstruct a complex network of drug−target relationships. As the data included many targets of allosteric modulators, the model may become a useful tool for the identification of allo-network drugs in the future.

Table 5. Top Results for CCHTS of Compound 11 in 170 Assays on Human Targets[a]

$p_1(m_j)$	STD TYPE MEASSURE	ASSAY ID	TARGET
1.00	K_i (nM)	751927	nitric-oxide synthase (bNOS), brain
0.98	$-\log(IC_{50})$ (nM)	751279	
0.97	$-\log(IC_{50})$ (nM)	750652	
0.98	$-\log(IC_{50})$ (nM)	892679	
0.98	$-\log(IC_{50})$ (nM)	833562	
0.90	$-\log(IC_{50})$ (nM)	751928	
0.89	inhibition (%)	752269	
0.89	$-\log(IC_{50})$ (nM)	751281	
0.87	$-\log(IC_{50})$ (nM)	750653	
0.87	$-\log(IC_{50})$ (nM)	751652	
0.85	$-\log(IC_{50})$ (nM)	750244	
0.85	$-\log(IC_{50})$ (nM)	751653	
0.84	$-\log(IC_{50})$ (nM)	751280	
0.84	K_i (nM)	843812	
0.81	inhibition (%)	752270	
0.81	inhibition (nM)	752268	
0.79	$-\log(IC_{50})$ (nM)	829483	
0.77	$-\log(IC_{50})$ (nM)	751278	
0.73	$-\log(IC_{50})$ (nM)	751656	
0.73	K_i (nM)	752276	
0.99	$-\log(IC_{50})$ (nM)	717365	MGluR 2
0.98	$-\log(IC_{50})$ (nM)	717366	
0.98	$-\log(IC_{50})$ (nM)	717236	MGluR 3
0.88	K_i (nM)	876081	GABA receptor gamma-2 subunit
0.88	K_i (nM)	682643	
0.88	K_i (nM)	876081	GABA receptor beta-2 subunit
0.88	K_i (nM)	682643	
0.97	$-\log(IC_{50})$ (nM)	876082	CAKI-1 (Kidney carcinoma cells)
0.97	$-\log(IC_{50})$ (nM)	843814	sodium channel protein type II alpha subunit
0.96	$-\log(IC_{50})$ (nM)	687680	HT-29 (Colon adenocarcinoma cells)
0.88	K_i (nM)	617201	serotonin 2a (5-HT2a) receptor
0.88	K_i (nM)	652074	beta-2 adrenergic receptor
0.88	K_i (nM)	748592	muscarinic acetylcholine receptor M2
0.82	$-\log(IC_{50})$ (nM)	829924	melanin-concentrating hormone receptor 1
0.78	EC_{50} (nM)	1613870	nuclear factor NF-kappa-B p105 subunit

[a] $p_1(m_j)$ is the probability with which the model predicts a value of the measure higher than the cutoff for compound **11**

3. METHODS

3.1. Computational Methods. *3.1.1. CHEMBL Data Set.* We downloaded >8000 multiplexing assay end points (results of multiple assays) from the public database CHEMBL.[66] A subset of 3548 results of assays (statistical cases) was used to train and validate the model. The second part of the >8000 initial cases containing 4671 positive cases and no negative cases was used to simulate an "in silico"HTS experiment.

3.1.2. The Moving Averages Model. The core of the model are the scores $S_i(c_j)$ and the kth molecular descriptors D^i_k of a given ith compound d_i and the deviation terms $\Delta D^i_k(c_j) = D^i_k - \langle D^i_k(c_j)\rangle$. The model has the following general form:

$$\begin{aligned} S_i(c_j) &= a_0 + \sum_{k=0}^{k=5} {}'a_k {}'S^k_i + \sum_{j=2}^{j=5} {}''a_{jk} {}''S_i{}^k(c_j) \\ &= a_0 + \sum_{k=0}^{k=5} {}'a_k p(c_l) D^i_k + \sum_{j=2}^{j=5}\sum_{k=0}^{k=5} {}''a_{jk}\Delta D^i_k(c_j) \\ &= a_0 + \sum_{k=0}^{k=5} {}'a_k p(c_l) D^i_k \\ &\quad + \sum_{j=2}^{j=5}\sum_{k=0}^{k=5} {}''a_{jk}[D^i_k - p(c_j)\langle D^i_k(c_j)\rangle] \end{aligned} \tag{4}$$

The output dependent variable is $S_i(c_j) = S_i(c_1, c_2, c_3, c_4, c_5,) = S_i(c_l, a_u, o_t, t_e, s_x)$. The variable $S_i(c_j)$ is a numerical score of the biological activity of the ith, drug annotated as d_i, in the jth assay carried out under the set of conditions c_j. Our hypothesis is H_0: we can calculate the output $S_i(c_j)$ as a linear combination of scores. We have two types of scores. The first type are the scores ${}'S^k_i = {}'a_k p(c_l)^i D_k$ that account for the quality of data $p(c_l)$ and for contributions of the kth molecular descriptors to the final activity score $S_i(c_j)$. In fact, we used the probability $p(c_1) = 1.0$, 0.75, or 0.5 for data curated in CHEMBL database at an expert, intermediate, or autocuration level, respectively. The second type are scores ${}''S^k_i(c_{j>1}) = {}''a_k\Delta D^i_k(c_j)$ for the contributions of deviations $\Delta D^i_k(c_j) = (D^i_k - \langle D^i_k(c_j)\rangle)$ of the descriptors of d_i from the average of those of active molecules $A_i(c_j) = 1$ for different c_j. In general, c_j refers to different multiplexing assay conditions, for example, targets, assays, cellular lines, organisms, organs, and so forth. In this sense, c_0 = is the accuracy of the data for this assay, $c_1 = a_u$ is the assay per se, $c_2 = o_t$ is the organism that expresses the target, $c_3 = t_e$ is the cellular or molecular target, and $c_5 = s_x$ is standard experimental measure of activity. Then, the parameter D^i_k and $\Delta D^i_k(c_j)$ are the input independent variables and $A_i(c_j) = 1$ is the input dependent variable. Herein, $\langle D^i_k(c_j)\rangle$ is the average of the kth descriptors D^i_k of all ith compounds considered as active ($A_i(c_j) = 1$) in an assay carried out under the set of conditions m_j. The parameters $\Delta D^i_k(c_j)$ are similar to the moving averages used in time series analysis for ARIMA models and others.[67,68] This type of moving average or deviation-like models has been used before to solve different problems in QSAR.[67,68] It means that, first, we sum the values of D^i_k for all the n_j drugs with $A_i(c_j) = 1$ in the assay carried out in the conditions c_j. Next, we divide this sum by the number of compounds n_j that fulfill this condition.

$$\langle D^i_k(c_j)\rangle = \frac{1}{n_j}\sum_{i=1}^{i=n_j} D^i_k(c_j) \tag{5}$$

In order to find the mx-QSAR model, we used the Linear Discriminant Analysis (LDA) technique implemented in the STATISTICA 6.0 software package.[69] In this model, we used only one molecular descriptor π^i_5. This is the spectral moment or order $k = 5$ calculated with MI. We did not use low-order moments $k = 0$, 1, 2, 3, and 4. Accordingly, the general equation is

$$\begin{aligned} S_i(c_j) &= a_0 + {}'\alpha_5 {}'S_i{}^5(c_l) + \sum_{j=2}^{j=5} {}''a_{jk} S_i{}^5(c_j) \\ &= a_0 + {}'a_5 p(c_l)\pi^i_5 + \sum_{j=2}^{j=5} {}''a_{jk}\Delta\pi^i_5(c_j) \\ &= a_0 + {}'a_k p(c_l)\pi^i_5 + \sum_{j=2}^{j=5}\sum_{k=0}^{k=5} {}''a_{jk}[\pi^i_5 - p(c_j)\langle\pi^i_5(c_j)\rangle] \end{aligned} \tag{6}$$

3.2. Experimental Methods. *3.2.1. Synthesis of 1,3-Rasagiline Derivatives.* The compounds (**5**−**12**) were synthesized according to the strategy given in Figure 2 (scheme 1). As shown in this scheme, they were synthesized from the hidroxy mono- or dipropargylaminoindans (**1**−**4**), previously described by us, and prepared following

dx.doi.org/10.1021/cn400111n | ACS Chem. Neurosci. 2013, 4, 1393−1403

procedures described in the literature.[28] Please see details about the techniques used for the characterization of compounds and the results obtained (NMR and IR spectra) in the Supporting Information.

3.2.2. Carbamylation of 1,3-Rasagiline Derivatives. To a stirred and ice-cooled solution of **1**, **2**, **3**, or **4** (0.43 mmol) in acetonitrile (5 mL) was added the corresponding N,N-dialkylcarbamyl chloride (0.73 mmol), followed by a dropwise addition of NaH (60% in oil, 0.56 mmol). The reaction mixture was stirred for 24 h at room temperature under argon. After evaporation of the solvent in vacuo, water (10 mL) was added and extracted with ether (3 × 10 mL). The organic phase was washed with dilute KOH (pH 10−11), dried, and evaporated to dryness in vacuo. Purification was afforded by column chromatography (hexane/EtOAc 4:1).

3.2.3. Identification of 1,3-Rasagiline Derivative Carbamates. Results obtained after spectroscopic and analytical chemistry processing of the new compounds are given as follows (see more details in the Supporting Information, section SM5).

Compound **5**. (±)-*cis*-3-(*N*-Propargylamino)-1-indanyl dimethylcarbamate (**5**) was obtained as a yellow solid (40 mg, yield 32%). Mp 73−75 °C. IR ν = 3218, 2920, 1701, 1342, 1182, 1042 cm^{-1}. ^1H NMR (300 MHz, $CDCl_3$) δ = 7.44−7.27 (m, 4H, Harom), 5.96−5.91 (m, 1H, 1-H), 4.24 (t, 1H, J = 6.4 Hz, 3-H), 3.48 (d, 2H, J = 2.4 Hz, CH_2), 2.94−2.85 (m, 7H, 2 × CH_3, 2α-H), 2.19−2.17 (m, 1H, CH), 1.95−1.86 (m, 2H, 2β-H, D_2O exch., NH) ppm. ^{13}C NMR (75 MHz, $CDCl_3$) δ = 156.47 (CO), 144.32 (C-7a), 141.36 (C-3a), 128.44, 128.19, 125.43, and 124.39 (CHarom), 82.12 (C≡CH), 76.28 (C≡CH), 71.58 (C-1), 59.36 (C-3), 40.91 (CH_2), 36.47 (CH_3), 36.10 (C-2), 35.98 (CH_3). MS (EI): *m*/*z* (%) 261 (2) [M+3]+, 186 (2) [(M-1)-carbamate]+, 130 (47), 116 (95). Anal. Calcd. for $C_{15}H_{18}N_2O_2$ (258.32): C, 69.74; H, 7.02; N, 10.84. Found: C, 69.51; H, 7.17; N, 11.02.

Compound **6**. (±)-*cis*-3-(*N*-Propargylamino)-1-indanyl diethylcarbamate (**6**) was obtained as a white solid (50 mg, yield 41%).[6] Mp 52−54 °C. IR ν = 3302, 2974, 1685, 1475, 1423, 1169, 1066 cm^{-1}. ^1H NMR (300 MHz, $CDCl_3$) δ = 7.44−7.27 (m, 4H, Harom), 6.03 (t, 1H, J = 6.2 Hz, 1-H), 4.29 (t, 1H, J = 6.3 Hz, 3-H), 3.54−3.53 (m, 2H, CH_2), 3.34−3.23 (m, 4H, 2 × CH_2CH_3), 3.01−2.91 (m, 1H, 2α-H), 2.49−2.23 (m, 1H, CH), 1.90 (dt, 1H, *J* = 13.4, 5.6 Hz, 2β-H), 1.63 (br. s, 1H, D_2O exch., NH), 1.16−1.14 (m, 6H, 2 × CH_2CH_3) ppm. ^{13}C NMR (75 MHz, $CDCl_3$) δ = 155.74 (CO), 144.24 (C-7a), 141.46 (C-3a), 128.74, 128.15, 125.29, and 124.32 (CHarom), 82.08 (C≡CH), 75.84 (C≡CH), 71.56 (C-1), 59.32 (C-3), 41.85 and 41.27 (2 × CH_2CH_3), 40.93 (CH_2), 36.09 (C-2), 14.16 and 13.56 (2 × CH_2CH_3) ppm. MS (FAB): *m*/*z* (%) 288 (83) [M+2]+, 287 (51) [M+1]+, 286 (4) [M]+, 231 (82), 154 (46), 137 (60), 115 (24). Anal. Calcd. for $C_{17}H_{22}N_2O_2$ (286.37): C, 71.30; H, 7.74; N, 9.78. Found: C, 71.02; H, 7.88; N, 9.81.

Compound **7**. (±)-*trans*-3-(*N*-Propargylamino)-1-indanyl dimethylcarbamate (**7**) was obtained as a yellow oil (54 mg, yield 43%). IR ν = 3287, 2928, 1691, 1392, 1179, 1047 cm^{-1}. ^1H NMR (300 MHz, CDCl3) δ = 7.49−7.29 (m, 4H, Harom), 6.22 (dd, 1H, J = 6.6, 4.1 Hz, 1-H), 4.62 (dd, 1H, J = 6.3, 5.0 Hz, 3-H), 3.52 (m, 2H, CH_2), 2.96−2.94 (m, 6H, 2 × CH_3), 2.48−2.30 (m, 2H, 2α-H, 2β-H), 2.27 (t, 1H, J = 2.4 Hz, CH), 1.70 (br. s, 1H, D_2O exch., NH) ppm. ^{13}C NMR (75 MHz, $CDCl_3$) δ = 156.96 (CO), 145.23 (C-7a), 143.04 (C-3a), 129.32, 128.62, 126.65, and 124.71 (CHarom), 82.48 (C≡CH), 76.32 (C≡CH), 72.12 (C-1), 60.01 (C-3), 41.61 (CH_2), 36.82 (CH_3), 36.50 (C-2), 36.36 (CH_3). MS (ESI): *m*/*z* (%) 259 (7) [M+3]+, 204 (7) [(M-1)-propargylamine]+, 115 (100). Anal. Calcd. for $C_{15}H_{18}N_2O_2$ (258.32): C, 69.74; H, 7.02; N, 10.84. Found: C, 69.63; H, 7.05; N, 10.97.

Compound **8**. (±)-*trans*-3-(*N*-Propargylamino)-1-indanyl diethylcarbamate (**8**) was obtained as a yellow oil (32 mg, yield 26%). IR ν = 3292, 2972, 1685, 1422, 1269, 1168, 1063 cm^{-1}. ^1H NMR (300 MHz, CDCl3) δ = 7.41−7.27 (m, 4H, Harom), 6.26 (dd, 1H, J = 6.5, 4.3 Hz, 1-H), 4.62 (dd, 1H, J = 6.4, 4.9 Hz, 3-H), 3.54−3.53 (m, 2H, CH_2), 3.38−3.15 (m, 4H, 2 × CH_2CH_3), 2.46−2.29 (m, 2H, 2α-H, 2β-H), 2.27 (t, 1H, J = 2.3 Hz, CH), 1.80 (br. s., 1H, D_2O exch., NH), 1.20−1.08 (m, 6H, 2 × CH_2CH_3). ^{13}C NMR (75 MHz, $CDCl_3$) δ = 155.90 (CO), 144.80 (C-7a), 141.90 (C-3a), 128.84, 128.23, 125.76, and 124.34 (CHarom), 82.11 (C≡CH), 77.15 (C≡CH), 71.72 (C-1), 59.66 (C-3), 42.21 and 41.76 (2 × CH_2CH_3), 41.14 (CH_2), 36.12 (C-2), 14.08 and 13.63 (2 × CH_2CH_3). MS (ESI): *m*/*z* (%) 288 (7) [M+2]+, 287 (100) [M+1]+, 232 (50) [M+-propargylamine], 115 (58). Anal. Calcd. for $C_{17}H_{22}N_2O_2$ (286.37): C, 71.30; H, 7.74; N, 9.78. Found: C, 71.12; H, 7.92; N, 9.90.

Compound **9**. (±)-*cis*-3-(*N*,*N*-Dipropargylamino)-1-indanyl dimethylcarbamate (**9**) was obtained as a yellow oil (70 mg; 66%). IR ν = 3288, 2932, 1394, 1182, 1047 cm^{-1}. ^1H NMR (300 MHz, CDCl3) δ = 7.45−7.28 (m, 4H, Harom), 5.96 (t, 1H, J = 6.7 Hz, 1-H), 4.54 (t, 1H, J = 7.2 Hz, 3-H), 3.56−3.42 (AB system, 2H, J = 16.8 Hz, CH_2), 3.55−3.41 (AB system, 2H, *J* = 16.8 Hz, CH_2), 2.94−2.87 (m, 6H, 2 × CH_3), 2.83−2.73 (m, 1H, 2α-H), 2.21 (t, 2H, *J* = 2.2 Hz, 2 × CH), 2.17−2.08 (m, 1H, 2β-H). ^{13}C NMR (75 MHz, $CDCl_3$) δ = 156.81 (CO), 143.07 (C-7a), 141.75 (C-3a), 129.26, 128.69, 125.33, and 125.28 (CHarom), 80.80 (2 × C≡CH), 76.33 (C-1), 73.12 (2 × C≡CH), 65.15 (C-3), 39.40 (2 × CH_2), 36.83 and 36.29 (2 × CH_3), 34.02 (C-2). MS (FAB): *m*/*z* (%) 298 (11) [M+2]+, 297 (57) [M+1]+, 296 (4) [M]+, 295 (13) [M-1]+, 208 (100) [(M-1)+-carbamate], 115 (83). Anal. Calcd. for $C_{18}H_{20}N_2O_2$ (296.36): C, 72.95; H, 6.80; N, 9.45. Found: C, 73.18; H, 6.72; N, 9.49.

Compound **10**. (±)-*cis*-3-(*N*,*N*-Dipropargylamino)-1-indanyl diethylcarbamate (**10**) was obtained as an oil (60 mg, yield 51%). IR ν = 3290, 2973, 1687, 1423, 1268, 1168 cm^{-1}. ^1H NMR (300 MHz, CDCl3) δ = 7.46−7.27 (m, 4H, Harom), 6.01 (t, 1H, *J* = 6.6 Hz, 1-H), 4.56 (t, 1H, *J* = 7.2 Hz, 3-H), 3.57−3.44 (AB system, 2H, *J* = 16.6 Hz, CH_2), 3.56−3.43 (AB system, 2H, *J* = 16.8 Hz, CH_2), 3.23−3.18 (m, 4H, 2 × CH_2CH_3), 2.79 (dt, 1H, J = 15.1, 7.4 Hz, 2α-H), 2.22 (t, 2H, *J* = 2.5 Hz, 2 × CH), 2.18−2.09 (m, 1H, 2β-H), 1.15−1.09 (m, 6H, 2 × CH_2CH_3) ppm. ^{13}C NMR (75 MHz, $CDCl_3$) δ = 156.16 (CO), 143.02 (C-7a), 141.96 (C-3a), 129.24, 128.72, 125.40, and 125.30 (CHarom), 80.83 (2 × C≡CH), 75.99 (2 × C≡CH), 73.13 (C-1), 65.19 (C-3), 42.26 and 41.65 (2 × CH_2CH_3), 39.44 (2 × CH_2), 34.00 (C-2), 14.54 and 13.99 (2 × CH_2CH_3). MS (FAB): *m*/*z* (%) 325 (73) [M+1]+, 324 (4) [M]+, 323 (10) [M-1]+, 288 (27), 208 (100) [(M-1)+-carbamate], 154 (17), 137 (24), 115 (91). Anal. Calcd. for $C_{20}H_{24}N_2O_2$ (324.42): C, 74.04; H, 7.46; N, 8.64. Found: C, 73.86; H, 7.71; N, 8.69.

Compound **11**. (±)-*trans*-3-(*N*,*N*-Dipropargylamino)-1-indanyl dimethylcarbamate (**11**) was obtained as a white solid (35 mg, yield 54%). Mp 108−110 °C. IR ν = 3289, 3218, 2918, 1681, 1393, 1179, 1040 cm^{-1}. ^1H NMR (300 MHz, CDCl3) δ = 7.41−7.27 (m, 4H, Harom), 6.10 (dd, 1H, J = 6.9, 3.3 Hz, 1-H), 4.75 (t, 1H, *J* = 6.3 Hz, 3-H), 3.49−3.34 (AB system, 2H, *J* = 16.8 Hz, CH_2), 3.48−3.33 (AB system, 2H, J = 16.8 Hz, CH_2), 2.86−2.76 (m, 6H, 2 × CH_3), 2.58 (dt, 1H, *J* = 12.8, 6.4 Hz, 2α-H), 2.20−2.11 (m, 3H, 2β-H, 2 × CH). ^{13}C NMR (75 MHz, $CDCl_3$) δ = 156.57 (CO), 143.63 (C-7a), 141.75 (C-3a), 129.14, 128.40, 125.87, and 125.24 (CHarom), 80.19 (2 × C≡CH), 77.40 (C-1), 72.86 (2 × C≡CH), 65.92 (C-3), 39.07 (2 × CH_2), 36.40 and 35.91 (2 × CH_3), 34.13 (C-2). MS (FAB): *m*/*z* (%) 298 (3) [M+2]+, 297 (16) [M+1]+, 231 (59), 208 (1) [(M-1)+-carbamate], 154 (90), 137 (100), 115 (6). Anal. Calcd. for $C_{18}H_{20}N_2O_2$ (296.36): C, 72.95; H, 6.80; N, 9.45. Found: C, 73.11; H, 6.72; N, 9.53.

Compound **12**. (±)-*trans*-3-(*N*,*N*-Dipropargylamino)-1-indanyl diethylcarbamate (**12**) was obtained as a white solid (86 mg, yield 74%). Mp 74−76 °C. IR ν = 3289, 3228, 2983, 1675, 1428, 1267, 1175 cm^{-1}. ^1H NMR (300 MHz, $CDCl_3$) δ = 7.46−7.26 (m, 4H, Harom), 6.21 (dd, 1H, *J* = 6.9, 3.6 Hz, 1-H), 4.81 (t, 1H, *J* = 6.4 Hz, 3-H), 3.55−3.42 (AB system, 2H, *J* = 16.8 Hz, CH2), 3.54−3.41 (AB system, 2H, *J* = 16.7 Hz, CH_2), 3.31−3.17 (m, 4H, 2 × CH_2CH_3), 2.66 (ddd, 1H, *J* = 14.5, 6.9, 5.5 Hz, 2α-H), 2.24 (t, 2H, J = 2.3 Hz, 2 × CH), 2.22−2.16 (m, 1H, 2β-H), 1.12−1.05 (m, 6H, 2 × CH_2CH_3) ppm. ^{13}C NMR (75 MHz, CDCl3) δ = 155.88 (CO), 143.49 (C-7a), 141.95 (C-3a), 129.03, 128.40, 125.73, and 125.28 (CHarom), 80.17 (2 × C≡CH), 77.07 (2 × C≡CH), 72.86 (C-1), 65.85 (C-3), 41.74 and 41.25 (2 × CH_2CH_3), 39.11 (2 × CH_2), 34.11 (C-2), 14.10 and 13.78 (2 × CH_2CH_3). MS (FAB): *m*/*z* (%) 326 (3) [M+2]+, 325 (28) [M+1]+, 278 (24), 231 (61), 154 (90), 137 (100). Anal. Calcd.

for $C_{20}H_{24}N_2O_2$ (324.42): C, 74.04; H, 7.46; N, 8.64. Found: C, 73.82; H, 7.65; N, 8.82.

3.2.4. Biological Assay of Neuroprotective Effects. The biological assay was carried out in three stages: (1) culture of rat cortical neurons, (2) measurement of neuronal viability, and (3) statistical analysis of results. In stage (1), we obtained neuronal cultures allowed to grow for 8−10 days until the microscope showed the existence of a dense neuronal network. In stage (2), we carried out the MTT reduction assay following the procedure previously described. Finally, in stage (3), data were expressed as mean ± SEM. Details of all the steps given can be found in our previous work, in the literature therein cited, and in the Supporting Information section SM6, of this work.[70]

■ ASSOCIATED CONTENT

Supporting Information

Tables SM1−SM4 contain detailed results of the computational studies. Section SM5 explains general methods used for the characterization of compounds and depicts figures of the NMR and IR characterization of these new compounds. This material is available free of charge via the Internet at http://pubs.acs.org.

■ AUTHOR INFORMATION

Corresponding Author

*E-mail: humberto.gonzalezdiaz@ehu.es (H.G.-D.); xerardo.garcia@usc.es (X.G.-M.).

Funding

The authors thank partial financial support from Xunta de Galicia (07CSA008203PR), Portuguese Fundação para a Ciência e a Tecnologia (FCT) and the European Social Fund (SFRH/BPD/63666/2009).

Notes

The authors declare no competing financial interest.

■ ACKNOWLEDGMENTS

All authors sincerely acknowledge the comments received from the editor Prof. Craig W. Lindsley who helped us to improve the final presentation of the manuscript. H.G.-D. thanks Prof. P. Csermely and Prof. R. Nussinov for providing us important bibliographic material about allo-network drugs.

■ REFERENCES

(1) Bettens, K., Sleegers, K., and Van Broeckhoven, C. (2013) Genetic insights in Alzheimer's disease. *Lancet Neurol. 12*, 92−104.

(2) Allegri, R. F., and Guekht, A. (2012) Cerebrolysin improves symptoms and delays progression in patients with Alzheimer's disease and vascular dementia. *Drugs Today 48* (Suppl. A), 25−41.

(3) Morales-Garcia, J. A., Susin, C., Alonso-Gil, S., Perez, D. I., Palomo, V., Perez, C., Conde, S., Santos, A., Gil, C., Martinez, A., and Perez-Castillo, A. (2013) Glycogen synthase kinase-3 inhibitors as potent therapeutic agents for the treatment of Parkinson disease. *ACS Chem. Neurosci. 4*, 350−360.

(4) Ludolph, A. C., Brettschneider, J., and Weishaupt, J. H. (2012) Amyotrophic lateral sclerosis. *Curr. Opin. Neurol. 25*, 530−535.

(5) Ha, A. D., and Fung, V. S. (2012) Huntington's disease. *Curr. Opin. Neurol. 25* (4), 491−498.

(6) Martin, L. J. (2012) Biology of mitochondria in neurodegenerative diseases. *Mol. Biol. Transl. Sci. 107*, 355−415.

(7) Howells, D. W., Sena, E. S., O'Collins, V., and Macleod, M. R. (2012) Improving the efficiency of the development of drugs for stroke. *Int. J. Stroke 7*, 371−377.

(8) Nurisso, A., Simoes-Pires, C., Martel, S., Cressend, D., Guillot, A., and Carrupt, P. A. (2012) How to increase the safety and efficacy of compounds against neurodegeneration? A multifunctional approach. *Chimia (Aarau) 66*, 286−290.

(9) Gaulton, A., Bellis, L. J., Bento, A. P., Chambers, J., Davies, M., Hersey, A., Light, Y., McGlinchey, S., Michalovich, D., Al-Lazikani, B., and Overington, J. P. (2012) ChEMBL: a large-scale bioactivity database for drug discovery. *Nucleic Acids Res. 40*, D1100−1107.

(10) Mok, N. Y., and Brenk, R. (2011) Mining the ChEMBL database: an efficient chemoinformatics workflow for assembling an ion channel-focused screening library. *J. Chem. Inf. Model. 51*, 2449−2454.

(11) Mueller, R., Rodriguez, A. L., Dawson, E. S., Butkiewicz, M., Nguyen, T. T., Oleszkiewicz, S., Bleckmann, A., Weaver, C. D., Lindsley, C. W., Conn, P. J., and Meiler, J. (2010) Identification of MGluR Subtype 5 Potentiators Using Virtual High-Throughput Screening. *ACS Chem. Neurosci. 1*, 288−305.

(12) Riera-Fernandez, P., Martin-Romalde, R., Prado-Prado, F. J., Escobar, M., Munteanu, C. R., Concu, R., Duardo-Sanchez, A., and Gonzalez-Diaz, H. (2012) From QSAR models of Drugs to Complex Networks: State-of-Art Review and Introduction of New Markov-Spectral Moments Indices. *Curr. Top. Med. Chem. 12*, 927−60.

(13) Prado-Prado, F., Garcia-Mera, X., Escobar, M., Sobarzo-Sanchez, E., Yanez, M., Riera-Fernandez, P., and Gonzalez-Diaz, H. (2011) 2D MI-DRAGON: a new predictor for protein-ligands interactions and theoretic-experimental studies of US FDA drug-target network, oxoisoaporphine inhibitors for MAO-A and human parasite proteins. *Eur. J. Med. Chem. 46*, 5838−5851.

(14) Helguera, A. M., Combes, R. D., Gonzalez, M. P., and Cordeiro, M. N. (2008) Applications of 2D descriptors in drug design: a DRAGON tale. *Curr. Top. Med. Chem. 8*, 1628−1655.

(15) Tetko, I. V., Gasteiger, J., Todeschini, R., Mauri, A., Livingstone, D., Ertl, P., Palyulin, V. A., Radchenko, E. V., Zefirov, N. S., Makarenko, A. S., Tanchuk, V. Y., and Prokopenko, V. V. (2005) Virtual computational chemistry laboratory–design and description. *J. Comput.-Aided Mol. Des. 19*, 453−463.

(16) Vilar, S., Cozza, G., and Moro, S. (2008) Medicinal chemistry and the molecular operating environment (MOE): application of QSAR and molecular docking to drug discovery. *Curr. Top. Med. Chem. 8*, 1555−1572.

(17) Estrada, E., and Uriarte, E. (2001) Quantitative structure-toxicity relationships using TOPS-MODE. 1. Nitrobenzene toxicity to Tetrahymena pyriformis. *SAR QSAR Environ. Res. 12*, 309−324.

(18) Estrada, E., Molina, E., and Uriarte, E. (2001) Quantitative structure-toxicity relationships using TOPS-MODE. 2. Neurotoxicity of a non-congeneric series of solvents. *SAR QSAR Environ. Res. 12*, 445−459.

(19) Estrada, E., Uriarte, E., Gutierrez, Y., and Gonzalez, H. (2003) Quantitative structure-toxicity relationships using TOPS-MODE. 3. Structural factors influencing the permeability of commercial solvents through living human skin. *SAR QSAR Environ. Res. 14*, 145−163.

(20) Katritzky, A. R., Perumal, S., Petrukhin, R., and Kleinpeter, E. (2001) Codessa-based theoretical QSPR model for hydantoin HPLC-RT lipophilicities. *J. Chem. Inf. Comput. Sci. 41*, 569−574.

(21) Katritzky, A. R., Oliferenko, A., Lomaka, A., and Karelson, M. (2002) Six-membered cyclic ureas as HIV-1 protease inhibitors: a QSAR study based on CODESSA PRO approach. Quantitative structure-activity relationships. *Bioorg. Med. Chem. Lett. 12*, 3453−3457.

(22) Katritzky, A. R., Kulshyn, O. V., Stoyanova-Slavova, I., Dobchev, D. A., Kuanar, M., Fara, D. C., and Karelson, M. (2006) Antimalarial activity: a QSAR modeling using CODESSA PRO software. *Bioorg. Med. Chem. 14*, 2333−2357.

(23) Marrero-Ponce, Y., J., C.-G., Olazabal, E., Serrano, H. S., Morales, A., Castañedo, N., Ibarra-Velarde, F., Huesca-Guillen, A., Jorge, E., del Valle, A., Torrens, F., and Castro, E. A. (2004) TOMOCOMD-CARDD, a novel approach for computer-aided 'rational' drug design: I. Theoretical and experimental assessment of a promising method for computational screening and in silico design of new anthelmintic compounds. *J. Comput.-Aided Mol. Des. 18*, 615−634.

(24) Marrero-Ponce, Y., Casanola-Martin, G. M., Khan, M. T., Torrens, F., Rescigno, A., and Abad, C. (2010) Ligand-Based

Computer-Aided Discovery of Tyrosinase Inhibitors. Applications of the TOMOCOMD-CARDD Method to the Elucidation of New Compounds. *Curr. Pharm. Des. 16*, 2601−2624.
(25) Gonzalez-Diaz, H., Duardo-Sanchez, A., Ubeira, F. M., Prado-Prado, F., Perez-Montoto, L. G., Concu, R., Podda, G., and Shen, B. (2010) Review of MARCH-INSIDE & complex networks prediction of drugs: ADMET, anti-parasite activity, metabolizing enzymes and cardiotoxicity proteome biomarkers. *Curr. Drug Metab. 11*, 379−406.
(26) Gonzalez-Diaz, H., Romaris, F., Duardo-Sanchez, A., Perez-Montoto, L. G., Prado-Prado, F., Patlewicz, G., and Ubeira, F. M. (2010) Predicting drugs and proteins in parasite infections with topological indices of complex networks: theoretical backgrounds, applications, and legal issues. *Curr. Pharm. Des. 16*, 2737−2764.
(27) Gonzalez-Diaz, H., Prado-Prado, F., and Ubeira, F. M. (2008) Predicting antimicrobial drugs and targets with the MARCH-INSIDE approach. *Curr. Top. Med. Chem. 8*, 1676−1690.
(28) Gonzalez-Diaz, H., Prado-Prado, F., Garcia-Mera, X., Alonso, N., Abeijon, P., Caamano, O., Yanez, M., Munteanu, C. R., Pazos, A., Dea-Ayuela, M. A., Gomez-Munoz, M. T., Garijo, M. M., Sansano, J., and Ubeira, F. M. (2011) MIND-BEST: Web Server for Drugs and Target Discovery; Design, Synthesis, and Assay of MAO-B Inhibitors and Theoretical-Experimental Study of G3PDH Protein from Trichomonas gallinae. *J. Proteome Res. 10*, 1698−1718.
(29) Gonzalez-Diaz, H., Prado-Prado, F., Sobarzo-Sanchez, E., Haddad, M., Maurel Chevalley, S., Valentin, A., Quetin-Leclercq, J., Dea-Ayuela, M. A., Teresa Gomez-Munos, M., Munteanu, C. R., Jose Torres-Labandeira, J., Garcia-Mera, X., Tapia, R. A., and Ubeira, F. M. (2011) NL MIND-BEST: A web server for ligands and proteins discovery-Theoretic-experimental study of proteins of Giardia lamblia and new compounds active against Plasmodium falciparum. *J. Theor. Biol. 276*, 229−49.
(30) Marzaro, G., Chilin, A., Guiotto, A., Uriarte, E., Brun, P., Castagliuolo, I., Tonus, F., and Gonzalez-Diaz, H. (2011) Using the TOPS-MODE approach to fit multi-target QSAR models for tyrosine kinases inhibitors. *Eur. J. Med. Chem. 46*, 2185−92.
(31) Speck-Planche, A., Kleandrova, V. V., Luan, F., and Cordeiro, M. N. (2012) A ligand-based approach for the in silico discovery of multi-target inhibitors for proteins associated with HIV infection. *Mol. BioSyst. 8*, 2188−2196.
(32) Speck-Planche, A., Kleandrova, V. V., Luan, F., and Cordeiro, M. N. (2012) Chemoinformatics in anti-cancer chemotherapy: Multi-target QSAR model for the in silico discovery of anti-breast cancer agents. *Eur. J. Pharm. Sci. 47*, 273−279.
(33) Speck-Planche, A., Kleandrova, V. V., and Cordeiro, M. N. (2013) Chemoinformatics for rational discovery of safe antibacterial drugs: Simultaneous predictions of biological activity against streptococci and toxicological profiles in laboratory animals. *Bioorg. Med. Chem. 21*, 2727−32.
(34) Speck-Planche, A., Kleandrova, V. V., and Cordeiro, M. N. (2013) New insights toward the discovery of antibacterial agents: multi-tasking QSBER model for the simultaneous prediction of anti-tuberculosis activity and toxicological profiles of drugs. *Eur. J. Pharm. Sci. 48*, 812−818.
(35) Speck-Planche, A., Kleandrova, V. V., Luan, F., and Cordeiro, M. N. (2012) Rational drug design for anti-cancer chemotherapy: multi-target QSAR models for the in silico discovery of anti-colorectal cancer agents. *Bioorg. Med. Chem. 20*, 4848−4855.
(36) Speck-Planche, A., Kleandrova, V. V., Luan, F., and Cordeiro, M. N. (2011) Multi-target drug discovery in anti-cancer therapy: Fragment-based approach toward the design of potent and versatile anti-prostate cancer agents. *Bioorg. Med. Chem. 19*, 6239−6244.
(37) Garcia, I., Fall, Y., Gomez, G., and Gonzalez-Diaz, H. (2011) First computational chemistry multi-target model for anti-Alzheimer, anti-parasitic, anti-fungi, and anti-bacterial activity of GSK-3 inhibitors in vitro, in vivo, and in different cellular lines. *Mol. Diversity 15*, 561−567.
(38) Wiederkehr, C., Basavaraj, R., Sarrauste de Menthiere, C., Hermida, L., Koch, R., Schlecht, U., Amon, A., Brachat, S., Breitenbach, M., Briza, P., Caburet, S., Cherry, M., Davis, R., Deutschbauer, A., Dickinson, H. G., Dumitrescu, T., Fellous, M., Goldman, A., Grootegoed, J. A., Hawley, R., Ishii, R., Jegou, B., Kaufman, R. J., Klein, F., Lamb, N., Maro, B., Nasmyth, K., Nicolas, A., Orr-Weaver, T., Philippsen, P., Pineau, C., Rabitsch, K. P., Reinke, V., Roest, H., Saunders, W., Schroder, M., Schedl, T., Siep, M., Villeneuve, A., Wolgemuth, D. J., Yamamoto, M., Zickler, D., Esposito, R. E., and Primig, M. (2004) GermOnline, a cross-species community knowledgebase on germ cell differentiation. *Nucleic Acids Res. 32*, D560−567.
(39) Youdim, M. B., Wadia, A., Tatton, W., and Weinstock, M. (2001) The anti-Parkinson drug rasagiline and its cholinesterase inhibitor derivatives exert neuroprotection unrelated to MAO inhibition in cell culture and in vivo. *Ann. N.Y. Acad. Sci. 939*, 450−458.
(40) Gerets, H. H., Dhalluin, S., and Atienzar, F. A. (2011) Multiplexing cell viability assays. *Methods Mol. Biol. 740*, 91−101.
(41) Martinez-Romero, M., Vazquez-Naya, J. M., Rabunal, J. R., Pita-Fernandez, S., Macenlle, R., Castro-Alvarino, J., Lopez-Roses, L., Ulla, J. L., Martinez-Calvo, A. V., Vazquez, S., Pereira, J., Porto-Pazos, A. B., Dorado, J., Pazos, A., and Munteanu, C. R. (2010) Artificial intelligence techniques for colorectal cancer drug metabolism: ontology and complex network. *Curr. Drug Metab. 11*, 347−368.
(42) Hill, T., and Lewicki, P. (2006) *STATISTICS Methods and Applications. A Comprehensive Reference for Science, Industry and Data Mining*, Vol. *1*, StatSoft, Tulsa.
(43) Luan, F., Cordeiro, M. N., Alonso, N., Garcia-Mera, X., Caamano, O., Romero-Duran, F. J., Yanez, M., and Gonzalez-Diaz, H. (2013) TOPS-MODE model of multiplexing neuroprotective effects of drugs and experimental-theoretic study of new 1,3-rasagiline derivatives potentially useful in neurodegenerative diseases. *Bioorg. Med. Chem. 21*, 1870−1879.
(44) Garcia-Garcia, A., Galvez, J., de Julian-Ortiz, J. V., Garcia-Domenech, R., Munoz, C., Guna, R., and Borras, R. (2004) New agents active against Mycobacterium avium complex selected by molecular topology: a virtual screening method. *J. Antimicrob. Chemother. 53*, 65−73.
(45) Marrero-Ponce, Y., Castillo-Garit, J. A., Olazabal, E., Serrano, H. S., Morales, A., Castanedo, N., Ibarra-Velarde, F., Huesca-Guillen, A., Sanchez, A. M., Torrens, F., and Castro, E. A. (2005) Atom, atom-type and total molecular linear indices as a promising approach for bioorganic and medicinal chemistry: theoretical and experimental assessment of a novel method for virtual screening and rational design of new lead anthelmintic. *Bioorg. Med. Chem. 13*, 1005−1020.
(46) Marrero-Ponce, Y., Machado-Tugores, Y., Pereira, D. M., Escario, J. A., Barrio, A. G., Nogal-Ruiz, J. J., Ochoa, C., Aran, V. J., Martinez-Fernandez, A. R., Sanchez, R. N., Montero-Torres, A., Torrens, F., and Meneses-Marcel, A. (2005) A computer-based approach to the rational discovery of new trichomonacidal drugs by atom-type linear indices. *Curr. Drug Discovery Technol. 2*, 245−265.
(47) Casanola-Martin, G. M., Marrero-Ponce, Y., Khan, M. T., Ather, A., Sultan, S., Torrens, F., and Rotondo, R. (2007) TOMOCOMD-CARDD descriptors-based virtual screening of tyrosinase inhibitors: evaluation of different classification model combinations using bond-based linear indices. *Bioorg. Med. Chem. 15*, 1483−1503.
(48) Casanola-Martin, G. M., Marrero-Ponce, Y., Tareq Hassan Khan, M., Torrens, F., Perez-Gimenez, F., and Rescigno, A. (2008) Atom- and bond-based 2D TOMOCOMD-CARDD approach and ligand-based virtual screening for the drug discovery of new tyrosinase inhibitors. *J. Biomol. Screening 13*, 1014−1024.
(49) Casanola-Martin, G. M., Marrero-Ponce, Y., Khan, M. T., Khan, S. B., Torrens, F., Perez-Jimenez, F., Rescigno, A., and Abad, C. (2010) Bond-based 2D quadratic fingerprints in QSAR studies: virtual and in vitro tyrosinase inhibitory activity elucidation. *Chem. Biol. Drug Des. 76*, 538−545.
(50) Rodriguez-Soca, Y., Munteanu, C. R., Dorado, J., Pazos, A., Prado-Prado, F. J., and Gonzalez-Diaz, H. (2010) Trypano-PPI: a web server for prediction of unique targets in trypanosome proteome by using electrostatic parameters of protein-protein interactions. *J. Proteome Res. 9*, 1182−1190.

(51) Gonzalez-Diaz, H., Muino, L., Anadon, A. M., Romaris, F., Prado-Prado, F. J., Munteanu, C. R., Dorado, J., Pazos Sierra, A., Mezo, M., Gonzalez-Warleta, M., Garate, T., and Ubeira, F. M. (2011) MISS-Prot: web server for self/non-self discrimination of protein residue networks in parasites; theory and experiments in Fasciola peptides and Anisakis allergens. *Mol BioSyst. 7*, 1938−1955.
(52) Wang, M. D., Huang, Y., Zhang, G. P., Mao, L., Xia, Y. P., Mei, Y. W., and Hu, B. (2012) Exendin-4 improved rat cortical neuron survival under oxygen/glucose deprivation through PKA pathway. *Neuroscience 226*, 388−96.
(53) Ryu, S., Shin, J. S., Cho, Y. W., Kim, H. K., Paik, S. H., Lee, J. H., Chi, Y. H., Kim, J. H., and Lee, K. T. (2013) Fimasartan, Anti-hypertension Drug, Suppressed Inducible Nitric Oxide Synthase Expressions via Nuclear Factor-Kappa B and Activator Protein-1 Inactivation. *Biol. Pharm. Bull. 36*, 467−474.
(54) Lorrio, S., Gomez-Rangel, V., Negredo, P., Egea, J., Leon, R., Romero, A., Dal-Cim, T., Villarroya, M., Rodriguez-Franco, M. I., Conde, S., Arce, M. P., Roda, J. M., Garcia, A. G., and Lopez, M. G. (2013) Novel multitarget ligand ITH33/IQM9.21 provides neuro-protection in in vitro and in vivo models related to brain ischemia. *Neuropharmacology 67*, 403−411.
(55) Youdim, M. B. (2013) Multi target neuroprotective and neurorestorative anti-Parkinson and anti-Alzheimer drugs ladostigil and M30 derived from rasagiline. *Exp. Neurobiol. 22*, 1−10.
(56) Conn, P. J., Lindsley, C. W., and Jones, C. K. (2009) Activation of metabotropic glutamate receptors as a novel approach for the treatment of schizophrenia. *Trends Pharmacol. Sci. 30*, 25−31.
(57) Conn, P. J., Jones, C. K., and Lindsley, C. W. (2009) Subtype-selective allosteric modulators of muscarinic receptors for the treatment of CNS disorders. *Trends Pharmacol. Sci. 30*, 148−155.
(58) Conn, P. J., Christopoulos, A., and Lindsley, C. W. (2009) Allosteric modulators of GPCRs: a novel approach for the treatment of CNS disorders. *Nat. Rev. Drug Discovery 8*, 41−54.
(59) Engers, D. W., Niswender, C. M., Weaver, C. D., Jadhav, S., Menon, U. N., Zamorano, R., Conn, P. J., Lindsley, C. W., and Hopkins, C. R. (2009) Synthesis and evaluation of a series of heterobiarylamides that are centrally penetrant mGluR 4 (mGluR4) positive allosteric modulators (PAMs). *J. Med. Chem. 52*, 4115−4118.
(60) Csermely, P., Nussinov, R., and Szilágyi, A. (2013) From allosteric drugs to allo-network drugs: state of the art and trends of design, synthesis and computational methods. *Curr. Top. Med. Chem. 13*, 2−4.
(61) Szilágyi, A., Nussinov, R., and Csermely, P. (2013) Allo-network drugs: extension of the allosteric drug concept to protein-protein interaction and signaling networks. *Curr. Top. Med. Chem. 13*, 64−77.
(62) Menniti, F. S., Lindsley, C. W., Conn, P. J., Pandit, J., Zagouras, P., and Volkmann, R. A. (2013) Allosteric modulators for the treatment of schizophrenia: targeting glutamatergic networks. *Curr. Top. Med. Chem. 13*, 26−54.
(63) Csermely, P., Korcsmáros, T., Kiss, H. J., London, G., and Nussinov, R. (2013) Structure and dynamics of molecular networks: A novel paradigm of drug discovery: A comprehensive review. *Pharmacol Ther. 138*, 333−408.
(64) Farkas, I. J., Korcsmáros, T., Kovács, I. A., Mihalik, Á, Palotai, R., Simkó, G. I., Szalay, K. Z., Szalay-Beko, M., Vellai, T., Wang, S., and Csermely, P. (2011) Network-based tools for the identification of novel drug targets. *Sci. Signaling 4*, pt3.
(65) Nussinov, R., Tsai, C. J., and Csermely, P. (2011) Allo-network drugs: harnessing allostery in cellular networks. *Trends Pharmacol. Sci. 32*, 686−693.
(66) Heikamp, K., and Bajorath, J. (2011) Large-scale similarity search profiling of ChEMBL compound data sets. *J. Chem. Inf. Model. 51*, 1831−1839.
(67) Tenorio-Borroto, E., Penuelas Rivas, C. G., Vasquez Chagoyan, J. C., Castanedo, N., Prado-Prado, F. J., Garcia-Mera, X., and Gonzalez-Diaz, H. (2012) ANN multiplexing model of drugs effect on macrophages; theoretical and flow cytometry study on the cytotoxicity of the anti-microbial drug G1 in spleen. *Bioorg. Med. Chem. 20*, 6181−6194.
(68) Speck-Planche, A., Kleandrova, V. V., Luan, F., and Cordeiro, M. N. (2011) Multi-target drug discovery in anti-cancer therapy: fragment-based approach toward the design of potent and versatile anti-prostate cancer agents. *Bioorg. Med. Chem. 19*, 6239−6244.
(69) StatSoft Inc. (2002) *STATISTICA* (data analysis software system), version 6.0, www.statsoft.com, Statsoft Inc., Tulsa, OK.
(70) Mosmann, T. (1983) Rapid colorimetric assay for cellular growth and survival: application to proliferation and cytotoxicity assays. *J. Immunol. Methods 65*, 55−63.